SEISMIC RESPONSE OF BURIED PIPELINES

M. Novak and A. Hindy

SYNOPSIS

This paper examines the response of pipelines in a homogeneous medium and in two different media separated by a vertical boundary; fault crossing is not considered. It summarizes the research conducted at The University of Western Ontario. The study conducted is theoretical and formulated in terms of both deterministic and random vibrations. The focus is on dynamic soil-pipe interaction. Excitation by seismic waves travelling along the pipe under different angles of incidence is considered as well as random response to seismic loading which is not fully correlated.

RESUME

Cette communication examine la réponse des oléoducs dans un sol homogène et dans deux différents sols divisés par un plan vertical; la traverse de faille n'est pas considérée. On résume la recherche conduite à l'Université de Western Ontario sur l'interaction dynamique sol/tuyau. De plus amples détails sur certains aspects de cette recherche peuvent être trouvés dans les sources de références citées. L'étude conduite est théorique et formulée en terme de vibration déterminante et aléatoire. L'excitation par onde sismique parcourant le tuyau selon différents angles d'incidence est considérée de même que la réponse aléatoire aux charges sismiques qui n'entrent pas complètement en corrélation.

M. Novak obtained his Dh.D. from the Institute of Theoretical and Applied Mechanics, Prague and is currently a Professor at The University of Western Ontario, London, Canada. A. Hindy is a Ph.D. student at The University of Western Ontario under M. Novak's supervision.

INTRODUCTION

Buried pipelines are used to transport various substances such as oil, water or gas over great distances. In cities, they represent a vital part of the lifeline system whose failure can greatly contribute to the total damage and suffering resulting from an earthquake.

The study of the behaviour of buried pipelines in a seismic environment can be divided into three groups depending on the type of medium that surrounds the pipe: response of pipes in homogeneous medium, response in medium with horizontally varying properties and response of pipelines crossing a fault. The study of all these situations started relatively recently but the body of information on pipe behaviour as well as practical guidelines for design have been increasing (4,10,11,14,19,20,21,22,23,24).

This paper examines the response of pipelines in a homogeneous medium and in two different media separated by a vertical boundary; fault crossing is not considered. It summarizes the research conducted at The University of Western Ontario. More details on some aspects of this research can be found in Refs. (7,9,16,17). The study conducted is theoretical and formulated in terms of both deterministic and random vibrations. The focus is on dynamic soil-pipe interaction. Excitation by seismic waves travelling along the pipe under different angles of incidence is considered as well as random response to seismic loading which is not fully correlated.

SOIL REACTIONS AND PIPE STIFFNESS

The predicted response of a pipeline to seismic motion of the ground depends greatly on the definition of the relationship between the motion of the pipe and the soil reactions to this motion. In many of the studies, these reactions were derived from static considerations and damping was only estimated. However, buried pipes are fully embedded bodies and consequently the damping (imaginary) part of the total soil reaction is large and just as important as its stiffness (real) part. Gross errors in the estimation of pipe damping can lead to completely unrealistic predictions of the response. The difficulty, however, is that no completely satisfactory description of the soil reactions is available except for the plane strain case with deep embedment. Therefore, this case is discussed first.

Plane Strain Case With Deep Embedment

Assume linear viscoelasticity with material damping of the frequency independent type (hysteretic damping) and a rigid infinitely long pipe undergoing harmonic uniform vibration. Then, the soil reactions to this motion can be described by means of complex dynamic stiffness per unit length of the pipe,

$$k_u = G[S_{u1}(a_o,\nu,\tan\delta) + i\, S_{u2}(a_o,\nu,\tan\delta)] \qquad (1)$$

in which $a_o = R\omega/V_s$, where R = pipe outer radius, ω = frequency, $V_s = \sqrt{G/\rho}$ = shear wave velocity of soil, G = shear modulus of soil and ρ = mass density of soil; finally, ν = Poisson's ratio and δ = the loss angle (soil material damping). The latter is also defined as $\tan\delta = G_2/G_1$ where G_1 and G_2 are the real and imaginary parts of the complex shear modulus, respectively. For embedment $d \to \infty$, the dimensionless parameters S_u follow from mathematically accurate expressions given for both lateral and axial motions in Ref. 18. The real part of Eq. 1 represents soil stiffness; the imaginary (out-of-phase) part describes the damping. The damping part stems primarily from energy radiation (i.e. geometric damping).

Eq. 1 offers basic information about the soil reactions associated with rigid body motions. For cases involving pipe bending, axial deformations and finite embedment depths, a more comprehensive description of soil reactions is needed. Such a description should include stiffness and damping constants relating any two stations along the pipeline. Because no such data are readily available, the soil reactions are described approximately by combining the static solution due to Mindlin (13) with the dynamic plane strain solution (18). The procedure is described in more detail in (7).

For a lumped mass system shown in Fig. 1, the soil stiffness and soil damping matrices, $[K_s]$ and $[C_s]$, are obtained in the form

$$[K_s] = GS_{u1}(\nu,\frac{d}{R},a_o)\ell\,[B]$$

$$[C_s] = G\bar{S}_{u2}(\nu,\frac{d}{R})\ell\,\frac{R}{V_s}\,[B] \qquad (2)$$

where for the case of ten masses, the dimensionless matrix [B] common to both soil stiffness and soil damping is

$$[B] = \begin{bmatrix} 1.0 & -0.1753 & -0.0556 & -0.0327 & -0.0223 & -0.0163 & -0.0124 & -0.0099 & -0.0082 & -0.006 \\ & 1.0 & -0.1753 & -0.0556 & -0.0327 & & & & & \\ & & 1.0 & -0.1753 & -0.0556 & & & \text{etc.} & & \\ & & & 1.0 & -0.1753 & & & & & \\ & & \text{symmetric} & & 1.0 & & & & & \end{bmatrix}$$

(A much higher number of masses, up to about thirty was actually used in the analysis).

The analogous matrices describing the stiffness of the pipe, [K], are derived in terms of mechanics. To circumvent the need to consider pipe rotations explicitly, the pipe bending stiffness is defined as indicated in Fig. 1b).With the soil reactions and the pipe stiffness matrices available, a number of different situations can be examined.

PIPE RESPONSE TO TRAVELLING WAVES

The soil resistance to pipe motion is generated by the relative motion between the pipe and the soil, u_i, (Fig. 1a) while the pipe resistance derives from the absolute displacement, U_i. For a lumped mass system, the equations of motion are

$$[m]\{\ddot{U}\} + [C_s]\{\dot{U}\} + [K]\{U\} = [C_s]\{\dot{u}_g\} + [K_s]\{u_g\} \qquad (3)$$

in which $[m]$ = the diagonal mass matrix, $[C_s]$ = the soil damping matrix, $[K]$ = pipe stiffness matrix and $[K_s]$ = the soil stiffness matrix; $\{U\}$ = the vector of absolute displacements of the pipe and the ground displacement vector is

$$\{u_g\} = [u_{1g} \quad u_{2g} \quad \cdots \quad u_{Ng}]^T \qquad (4)$$

The dots indicate differentiation with respect to time.

Eq. 3 is formally the same for both lateral and axial vibrations; the difference is only in the stiffness and damping matrices and the components of ground motion.

The response is solved from Eq. 3 considering the seismic motion travelling along the pipe at different angles of incidence. It is assumed that the ground motion has the same time history in all types of waves and that it does not change along the pipe. (Attenuation of the motion was considered only in a few cases.) P- and S-waves are

considered and in each case the soil particle motion is resolved into two components: one in the axial direction and the other in the lateral direction. The former component causes axial stresses, the latter results in bending stresses.

A few methods including modal analysis were employed to obtain the solution. The best results were achieved using the Wilson-θ method (25) with $\theta = 1.4$.

The convergence of the numerical results appeared satisfactory for the number of lumped masses greater than 25. Therefore, this number was used in most cases.

The results are presented for a steel pipeline 137.16 cm in diameter and 548.6 m in length. The wall thickness is 1.11 cm. Free ends are assumed and embedment is taken as 15 diameters or variable. (The results are not too sensitive to the embedment depth.)

In most of the study, the time history of the ground motion is taken as equal to that measured during the San Fernando Valley Earthquake, 1971, at station 122, component S70E; rms ground acceleration = 0.361 m/s^2, peak acceleration = 2.657 m/s^2 and peak velocity = 0.3084 m/sec. The effect of other types of motion is considered in a few cases.

With these data, pipe displacements and stresses are established solving Eq. 3. An example of the stresses calculated is shown in Fig. 2 together with the time histories of the ground velocity and acceleration. When no soil-pipe interaction occurs, the pipe exactly follows the motion of the ground; in such a case the pipe axial stresses should be proportional to ground velocity and the bending stresses should be proportional to ground acceleration.

The degree of this agreement depends on the stiffness of the soil and the type of excitation. This is shown in Figs. 3 and 4 in which the peak (maximum) stresses are plotted for different types of waves and different angles of attack. For comparison, the pipe stresses calculated ignoring soil-pipe interaction are also plotted.

A number of observations can be drawn from Figs. 3 and 4:

For a P-wave, the maximum axial strain occurs at $\theta = 90°$, i.e. when the P-wave follows the direction of the pipe. The maximum bending strain occurs when $\theta = 50°$-$60°$. Soil-pipe interaction reduces the stresses. This reduction is greater for axial stress than for bending stress and increases with decreasing soil stiffness.

For an S-wave, maximum bending strain occurs at $\theta = 90°$ while maximum axial strain occurs at $\theta = 40 - 45°$. With stiff soils, the interaction effect is small in all cases.

With the mathematical model described, an extensive parametric study was conducted. The effects of soil stiffness, pipe stiffness, pipe length, embedment depth and other factors are described in (7,8). The model is also suitable for linked pipes.

The lumped mass model can also be used to study the seismic response of pipes crossing a vertical boundary between two soil media having different stiffnesses. The solution has to incorporate the waves reflected from the boundary. Examples of the envelopes of the peak stresses are shown in Figs. 5 and 6. The maximum stresses are plotted for a number of ratios of the shear wave velocities in the two media, V_{s2}/V_{s1}. The maximum stresses occur in the vicinity of the boundary and can exceed the values predicted ignoring soil-pipe interaction.

RESPONSE OF PIPELINES TO RANDOM GROUND MOTION

In the above approach, the ground motion was assumed to be transient but fully correlated. In this section, the pipe stresses are analyzed under the assumption that the ground motion is only partially correlated. The aim of this analysis is to establish whether this kind of excitation could produce pipe stresses in excess of those calculated under the usual assumption of full correlation of the ground motion. The importance of this question is best exemplified by the case of lateral response to fully correlated ground motion which approaches the pipe under zero angle of incidence, i.e. the wave front is parallel to the pipe axis. In such a case, no bending stresses occur. However, if the ground motion is not fully correlated, considerable bending stresses can be generated as are shown below.

This type of dynamic analysis is best formulated in terms of random vibration. This approach makes it possible to account for the loss of correlation with both the distance (separation) and frequency. Such a loss of correlation is indicated by some experimental evidence (1,2,3,12) and can be anticipated with respect to the properties of other random phenomena such as natural wind or, in general, turbulent flow.

Assume that the ground motion is homogeneous, i.e. statistically the same at all stations and described by the power spectrum of acceleration, $S_{\ddot{u}_g}(f)$. The cross-spectrum of ground accelerations at two points of the pipe, y_1 and y_2 can then be written as

$$S_{\ddot{u}_g}(y_1,y_2,f) = S_{\ddot{u}_g}(f)R(y_1,y_2,f) \tag{5}$$

in which the normalized cross-spectrum

$$R(y_1,y_2,f) = e^{-c\frac{rf}{V_s}} \tag{6}$$

where $r = |y_2-y_1|$ = horizontal separation, f = frequency, V_s/f = wave length; c = a constant depending on the distance from the epicentre, intensity of the earthquake, pathway and other characteristics of the earthquake.

The shape of the power spectrum, $S_{\ddot{u}_g}$, and the magnitude of the coefficient, c, can be established from experimental observations. The acceleration spectrum must be such that the corresponding displacement spectrum

$$S_{u_g}(\omega) = \frac{S_{\ddot{u}_g}(\omega)}{\omega^4} \tag{7}$$

is finite for $\omega \to 0$. Suitable shapes were found using optimization subroutines. The three spectra used in the parametric study are shown in Figs. 7 and 8.

Equation of Pipe Response and Its Solution

When formulating the equations of pipe response in terms of random vibration, a significant advantage can be taken of an observation derived from the parametric study of the lumped mass system. It was found that the effect of the off-diagonal soil stiffness and damping terms on the pipe response is quite small. Neglecting these off-diagonal terms, the equation of the pipe lateral motion can be written for a distributed system as

$$\mu \frac{\partial^2 U(y,t)}{\partial t^2} + G(S_{u1}+iS_{u2})U(y,t) + E_pI \frac{\partial^4 U(y,t)}{\partial y^4} + \lambda \frac{\partial U(y,t)}{\partial t}$$

$$= G(S_{u1}+iS_{u2})u_g(y,t) \tag{8}$$

in which μ = mass of the pipe per unit length, E_pI = bending stiffness of the pipe, λ = coefficient of pipe internal damping which can be neglected and $U(y,t)$ = the absolute displacement of the pipe; the soil reactions are described by means of parameters S and Eq. 1.

The advantage of this formulation is that a closed form solution of the random response can be obtained for some end conditions of the pipe. Because the stresses in the central part of a long pile are rather independent of the end conditions, guided ends are assumed; they yield very simple mode shapes,

$$\phi_j(y) = \cos(a_j \frac{y}{L}) \tag{9}$$

in which

$$a_j = (j-1)\pi, \qquad j = 1,2,3...$$

The first mode represents the rigid body motion. The undamped natural frequencies, ω_j, are given by Eqs. 10 and 11.

$$\omega_j = \psi_{b_j} \sqrt{\frac{GS_{u1}}{\mu}} \tag{10}$$

$$\psi_{b_j} = \sqrt{1 + \frac{\pi^4}{S_{u1}} \frac{E}{G} \frac{I}{L^4} (j-1)^4} \tag{11}$$

With the mode shapes and natural frequencies established, it is also possible to calculate the damping ratios associated with individual vibration modes. These modal damping ratios can be evaluated on the basis of an energy consideration outlined in Ref. 15. Integrating the work done by the damping forces W_j and relating this work to kinetic energy E_j, the modal damping ratios of buried pipes are

$$D_j = W_j/4\pi E_j$$

$$= \frac{\bar{S}_{u2}}{2\sqrt{\pi \bar{S}_{u1}}} \left(\frac{\rho_p}{\rho}\right)^{1/2} \frac{1}{\psi_{b_j}} \tag{12}$$

where $\bar{S}_{u1}$ and $\bar{S}_{u2}$ = constant soil stiffness and damping parameters, and ρ_p = average mass density of the pipe.

For the typical pipeline used in the previous section, the damping ratios turn out to be $D_1 = 125\%$, $D_2 = 119\%$, $D_3 = 110\% \ldots D_{15} = 50\%$. The damping of buried pipelines is obviously very high. This is of consequence for the further development of the random approach and also for other approximate solutions in which the modal damping ratios are only estimated.

Using modal analysis and the mode shapes given by Eq. 9, the mean square response is

$$\overline{U^2(y)} = \sum_{j=1}^{N} \sum_{k=1}^{N} \overline{\eta_j(t)\eta_k(t)}\, \phi_j(y)\phi_k(y) \tag{13}$$

in which $\overline{\eta_j(t)\eta_k(t)}$ = the covariance of generalized coordinates, $\eta(t)$, calculated from a general relation (5)

$$\overline{\eta_j(t)\eta_k(t)} = \int_0^\infty \alpha_k(i\omega)\alpha_j(-i\omega) S^g_{u_j u_k}(\omega)\, d\omega \tag{14}$$

in which $\alpha(i\omega)$, $\alpha(-i\omega)$ = the admittance function and its complex conjugate, respectively. Their evaluation and substitution into Eq. 14 yields, after integration and some other manipulations,

$$\overline{\eta_j(t)\eta_k(t)} =$$

$$\theta_{j,k}\int_0^\infty \frac{J_{j,k}(n)[S_{u1}^2(a_o)+S_{u2}^2(a_o)]S_{u_g}(\omega)d\omega}{[S_{u1}(a_o)\psi_{b_j}^2-(\frac{\rho_p}{\rho})\pi a_o^2+iS_{u2}(a_o)][S_{u1}(a_o)\psi_{b_k}^2-(\frac{\rho_p}{\rho})\pi a_o^2-iS_{u2}(a_o)]} \quad (15)$$

where

$$\theta_{j,k} = \frac{1}{[\int_0^1 \phi_j^2(y^1)dy^1][\int_0^1 \phi_k^2(y^1)dy^1]}$$

in which the joint acceptance function is

$$J_{j,k}(n) = \frac{n}{(n^2+a_j^2)}\{\frac{\sin(a_j-a_k)}{(a_j-a_k)} + \frac{\sin(a_j+a_k)}{(a_j+a_k)} + \frac{n}{(n^2+a_k^2)}[e^{-n}(\cos a_k+\cos a_j)-\cos a_j \cos a_k - 1]\} \quad (16)$$

(This step is described in more detail in Hindy, Ref. 8).

The joint acceptance function is a very important characteristic of the response and is shown in Fig. 9 in terms of the reduced dimensionless frequency, $n = cfL/V_s$, in which L = the length of the pipe.

Substitution of Eq. 15 into Eq. 13 yields the mean square of the bending moment at station y

$$\overline{M^2}(y) = (E_pI)^2 \sum_{j=1}^{N}\sum_{k=1}^{N} \overline{\eta_j(t)\eta_k(t)} \frac{d^2\phi_j(y)}{dy^2}\frac{d^2\phi_k(y)}{dy^2} \quad (17)$$

The expected peak value of the bending stress is

$$\bar{\hat{f}} = g\sqrt{\overline{M^2}}\ \frac{R}{I} \quad (18)$$

in which g = the peak factor (6). For the pipe used in the parametric study, g = 1.75 to 1.85.

The outlined approach differs from that usually applied with structures in that the off-diagonal terms, $\overline{\eta_j\eta_k}$ for $j \neq k$, are significant and cannot be neglected in the analysis. This is so because the damping of fully embedded pipes is very high as has already been shown.

An analogous approach can be formulated for the axial stresses of the pipes (9).

Examples of Numerical Results

Examples of the numerical results established by means of the random approach are shown in Figs. 10 and 11. The stresses are almost constant along the pipe except near the boundaries where they depend on the end condition. While the total motion is only slightly larger than the rigid body displacement, the resultant stresses can be quite high. The level of these stresses is governed by the degree of the ground motion correlation which is described by the magnitude of the parameter, c, (Eq. 6). The effect of this parameter can be seen from Fig. 12. The analysis of the limited experimental data available indicates that c should be smaller than 1 with 0.1 to 0.3 being typical values.

The spatial correlation can be expressed either by the coefficient, c, or by a physically more tangible measure, the correlation length, L. Integrating the correlation coefficient, the correlation length of ground displacement is found to be

$$L_d = \left(\frac{\sigma_{\ddot{u}_g}}{\sigma_{u_g}}\right)^2 \int_0^\infty \int_0^\infty e^{-c\frac{\omega r}{2\pi V_s}} \frac{S^n_{\ddot{u}_g}}{\omega^4} \, d\omega \, dr \tag{19}$$

The correlation length of ground acceleration is similarly

$$L_a = \int_0^\infty \int_0^\infty e^{-c\frac{\omega r}{2\pi V_s}} S^n_{\ddot{u}_g} \, d\omega \, dr \tag{20}$$

In Eqs. 19 and 20,

$$S^n_{\ddot{u}_g} = \frac{1}{\sigma^2_{\ddot{u}_g}} S_{\ddot{u}_g} \tag{21}$$

and is the normalized ground acceleration spectrum. The relation between the parameter, c, and the correlation length of the seismic ground motion is plotted in Fig. 13.

SUMMARY AND CONCLUSIONS

A theoretical study of seismic response of buried pipelines was conducted using two approaches: a lumped mass model excited by travelling seismic waves and a distributed model exposed to partially correlated random ground motion. An extensive parametric study yielded a number of practical conclusions:

Axial stresses in the pipe are much higher than bending stresses.

In a homogeneous medium, soil-pipe interaction reduces the pipe

stresses compared to those calculated ignoring interaction. This reduction is greater for axial stress than for bending stress but decreases with increasing stiffness of soil.

When the pipe crosses a boundary between two media, higher stresses occur in the vicinity of the boundary and can exceed those predicted ignoring soil-pipe interaction.

The effect of embedment depth and the off-diagonal terms in the stiffness and damping matrices describing the soil reactions are not very significant.

When the ground motion is not fully correlated, pipe stresses can be considerably increased; high bending stresses can occur with zero angle of incidence in which case no bending stress results from a fully correlated ground motion.

Further research into spatial correlation of seismic ground motions is desirable.

ACKNOWLEDGEMENT

The study was supported by a research grant from the National Research Council of Canada which is gratefully acknowledged.

REFERENCES

1. Aki, K. "Scattering of P Wave Under the Montana Lasa", Journal of Geophysical Research, Vol. 78, No. 8, 1973.

2. Berteussen, K.A., Christoffersson, A., Husebye, E.S. and Dahle, A. "Wave Scattering Theory in Analysis of P-Wave Anomalies at NORSAR and LASA", Geophysics J. Roy. Astr. Soc. 42,1975, 403-417.

3. Chernov, L.A. Wave Propagation in a Random Medium, McGraw-Hill, 1960.

4. "Earthquake Lifelines and the ASCE", Civil Engineering-ASCE, December 1973.

5. Clough, R.W. and Penzien, J. Dynamics of Structures, McGraw-Hill, 1975.

6. Davenport, A.G. "The Distribution of Largest Values of Random Function With Application to Gust Loading", Proceedings, Institution of Civil Engineering, London, Vol. 28, 1964, pp. 187-196.

7. Hindy, A. and Novak, M. "Earthquake Response of Underground Pipelines", University Report GEOT-1-1978, University of Western Ontario, London, Canada.

8. Hindy, A. "Seismic Response of Buried Pipelines", Ph.D. Thesis, University of Western Ontario, London, Ontario, February 1979.

9. Hindy, A. and Novak, M. "Response of Pipelines to Random Ground Motion", Journal of the Engineering Mechanics Division, ASCE (offered for publication).

10. Katayama, T., Kubo, K. and Sato, N. "Earthquake Damage to Water and Gas Distribution Systems", Proceedings of the U.S. National Conference on Earthquake Engineering, Ann Arbor, Michigan, EERI, 1975, pp. 396-405.

11. Kubo, K. "Behaviour of Underground Waterpipes During An Earthquake", Proceedings of the Fifth World Conference on Earthquake Engineering, Vol. 1, 569, Rome 1973.

12. Leslie, H.D., Porter, R.P. and Spindel, R.C. "Microearthquake Location Using a Maximum Likelihood Processor", Geophysics, Vol. 41, 1976, pp. 960-969.

13. Mindlin, R.D. "Displacements and Stresses Due to Nuclei of Strain in the Elastic Half-Space", Report of the Dept. of Civil Engineering and Engineering Mechanics, Columbia University, New York, N.Y., 1964.

14. Newmark, N.M. and Hall, W.J. "Pipeline Design to Resist Large Fault Displacement", Proceedings of the U.S. National Conference on Earthquake Engineering - 1975, June 1975, Ann Arbor, Michigan, pp. 416-425.

15. Novak, M. "Effect of Soil on Structural Response to Wind and Earthquake", Earthquake Engineering and Structural Dynamics, Vol. 3, 1974, 79-96.

16. Novak, M. and Hindy, A. "Seismic Response of Buried Pipelines", Proceedings of the Second Annual Engineering Mechanics Division Specialty Conference, ASCE, Rayleigh, North Carolina, May 1977.

17. Novak, M. and Hindy, A. "Dynamic Response of Buried Pipelines", Proceedings of the Sixth European Conference on Earthquake Engineering, Dubrovnik, Yugoslavia, September 1978.

18. Novak, M., Nogami, T. and Aboul-Ella, F. "Dynamic Soil Reactions for Plane Strain Case", Journal of the Engineering Mechanics Division, ASCE, August 1978.

19. Parmelee, R. and Ludtke, C. "Seismic Soil-Structure Interaction of Buried Pipelines", Proceedings of the U.S. National Conference on Earthquake Engineering, 1975, pp. 406-415.

20. Sakurai, A. and Takahashi, "Dynamic Stresses of Underground Pipelines During Earthquakes", Proceedings of the 4th World Conference on Earthquake Engineering, Santiago, Chile, Jan. 1969, Vol. 2, pp. B4-81 to B4-96.

21. Shinozuka, M. and Kawakami, H. "Underground Pipe Damages and Ground Characteristics", Proceedings of the ASCE Specialty Conference on Lifeline Earthquake Engineering, Los Angeles, August 1977, pp. 293-307.

22. Toki, K. and Takada, S. "Earthquake Response Analysis of Underground Tubular Structures", Bulletin of Disaster Prevention Research Institute, Vol. 24, 1974, Kyoto University.

23. Wang, L. and Cheng, K. "Seismic Response Behaviour of Buried Pipelines", ASME Annual Winter Convention, San Francisco, California, December 11-15, 1978.

24. Weidlinger, P. and Nelson, I. "Seismic Analysis of Lifelines With Interference Response Spectra", Grant Report No. 7, Prepared for National Science Foundation (RANN), Grant No. P76-9838, Weidlinger Associates, New York, June 1978.

25. Wilson, E.L., Farhoomand, I. and Bathe, K.J. "Nonlinear Dynamic Analysis of Complex Structures", Earthquake Engineering and Structural Dynamics, Vol. 1, 1973, pp. 241-252.

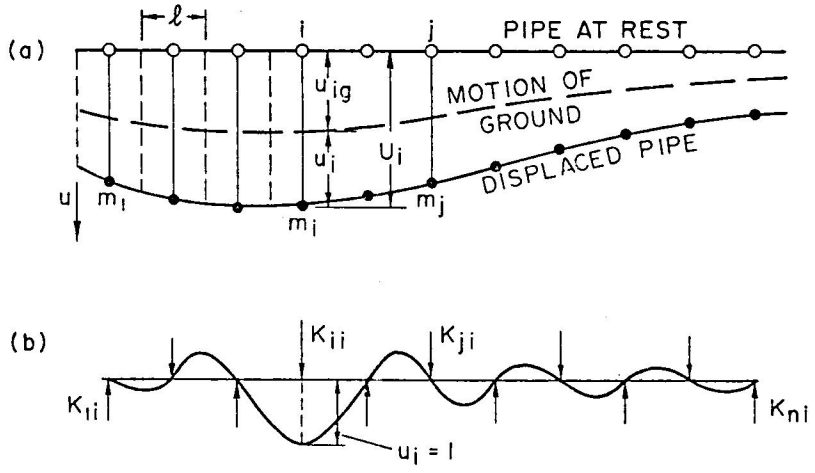

Figure 1 Lumped mass model of pipe.

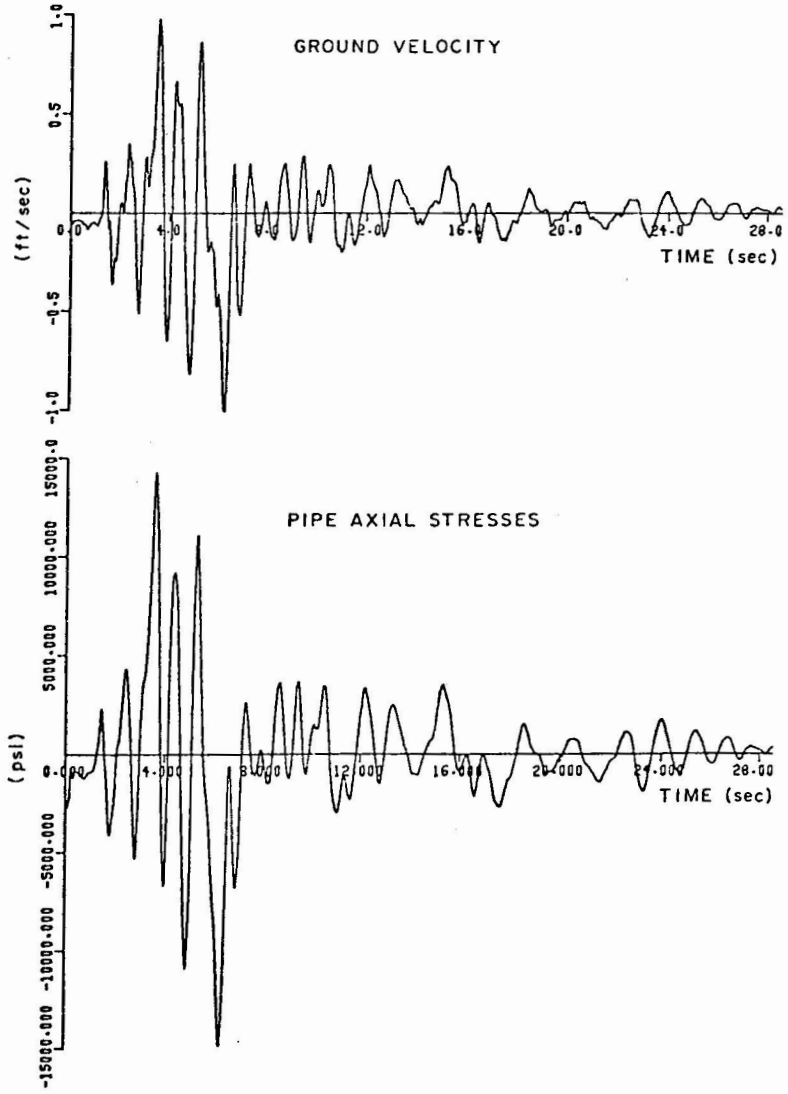

Figure 2(a) Time History of Ground Velocity of San Fernando Valley Earthquake (1971) and Corresponding Axial Stresses in Pipe.

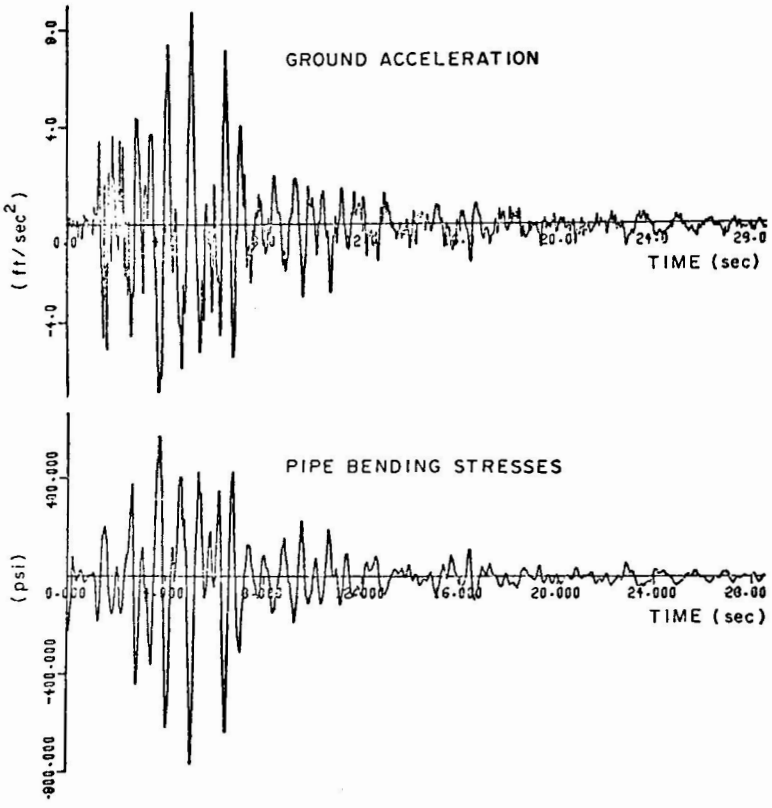

Figure 2(b) Time History of Ground Acceleration of San Fernando Valley Earthquake (1971) and Corresponding Bending Stresses in Pipe.

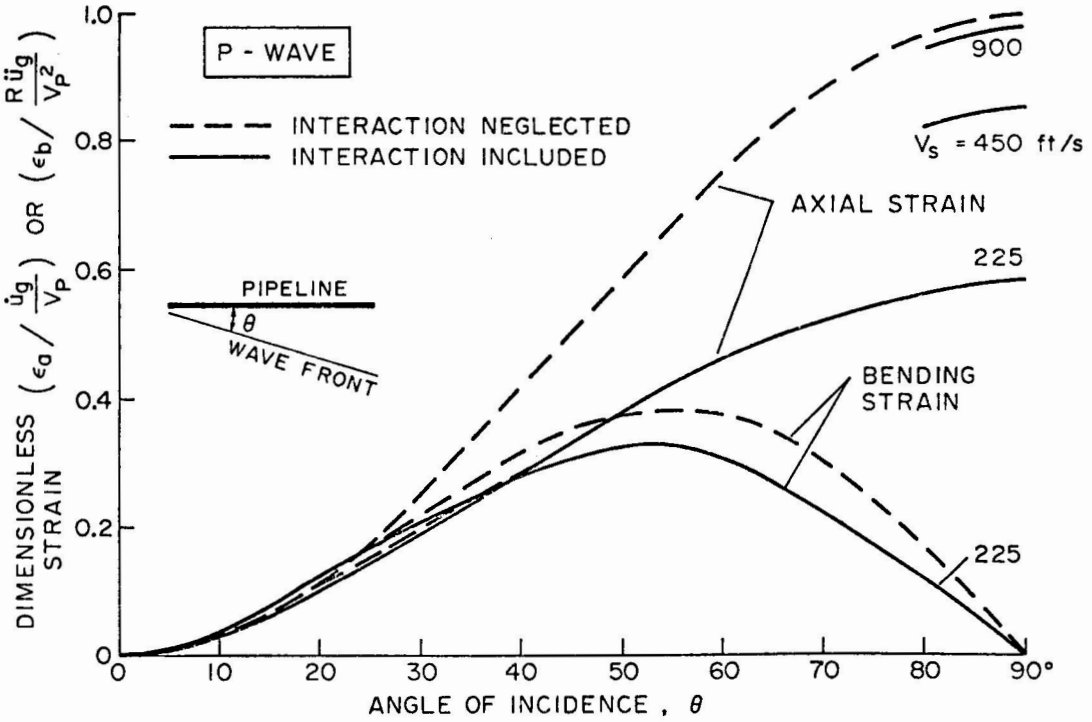

Figure 3 Variation of peak axial and bending strains in pipe with angle of incidence of P-wave.

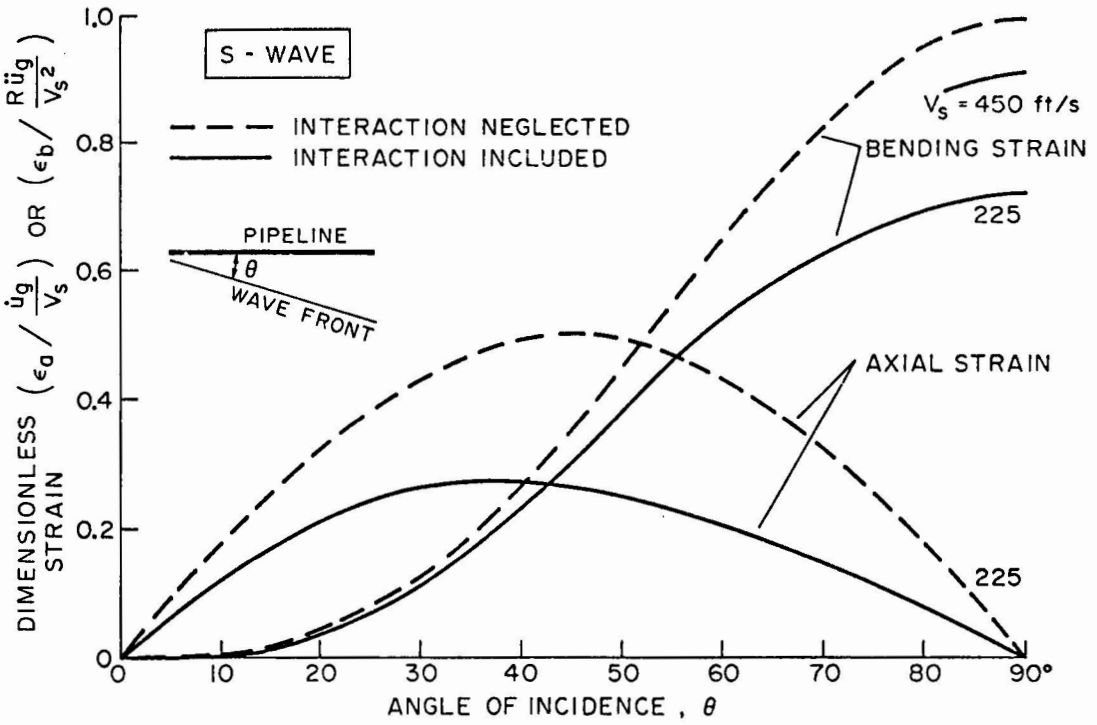

Figure 4 Variation of peak axial and bending strains in pipe with angle of incidence of S-wave.

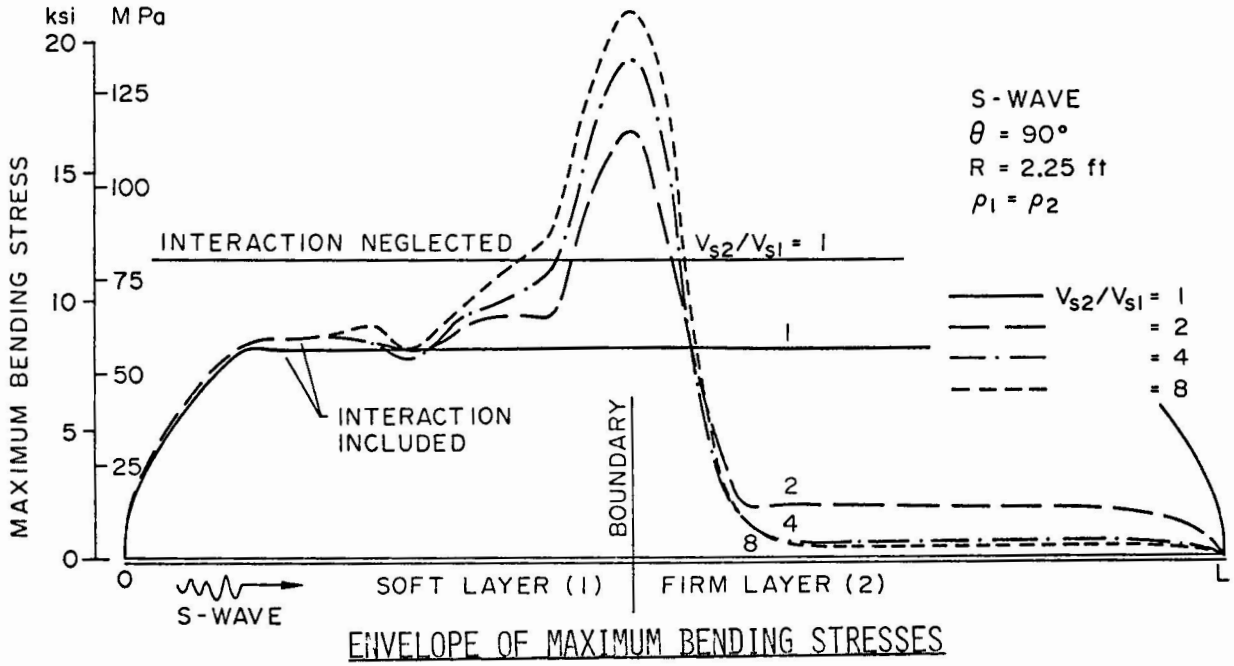

Figure 5 Maximum bending stresses in pipe due to S-wave propagating from soft soil to firm.

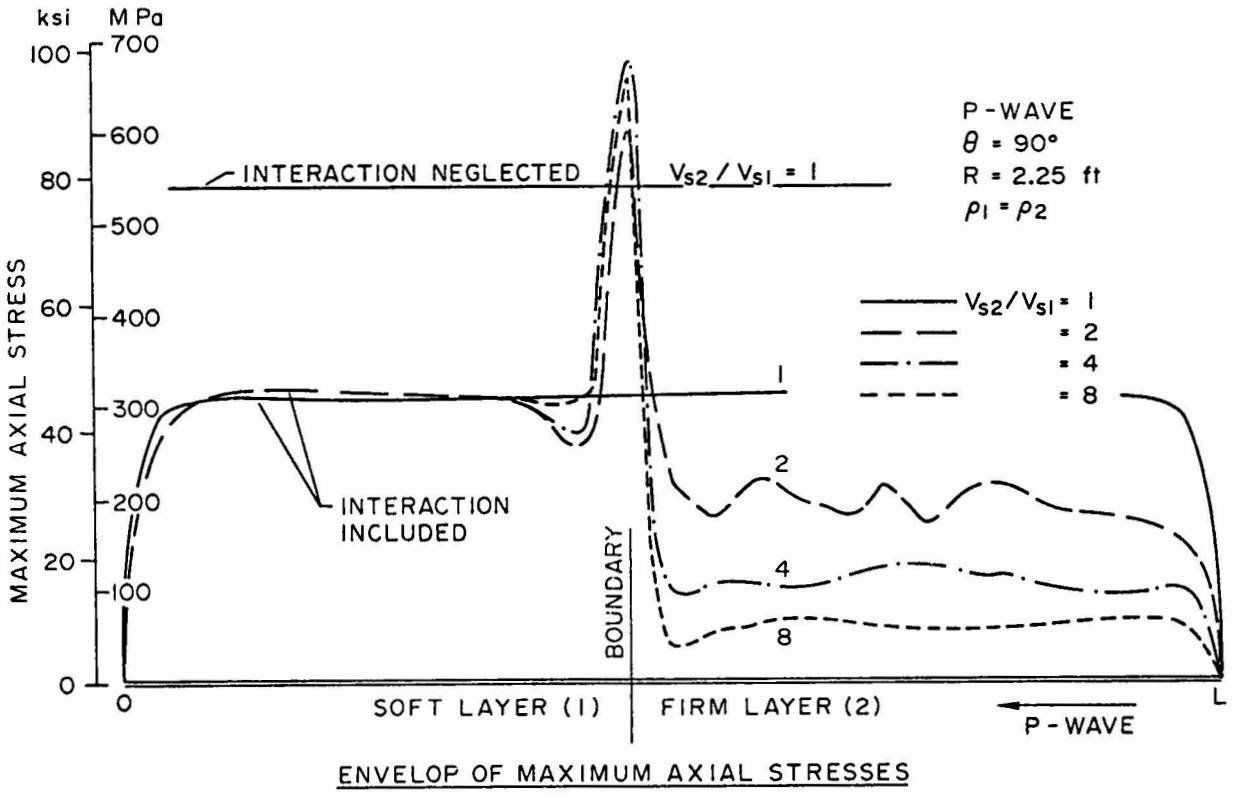

Figure 6 Maximum axial stresses in pipe due to P-wave propagating from firm soil to soft.

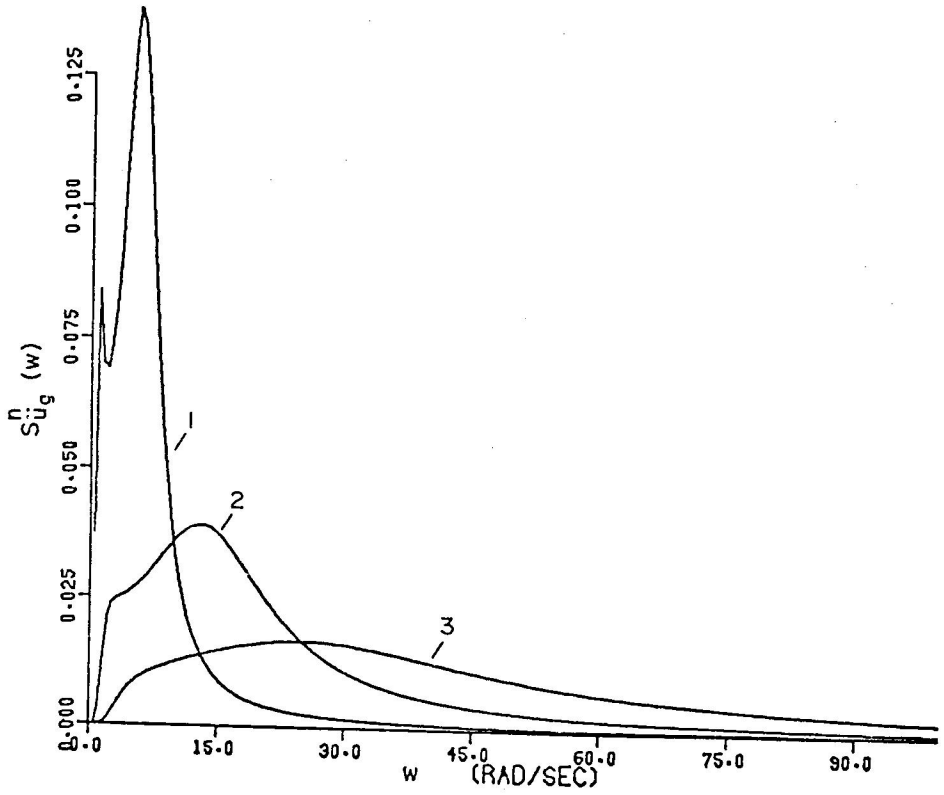

Figure 7 Normalized Spectra of Ground Acceleration.

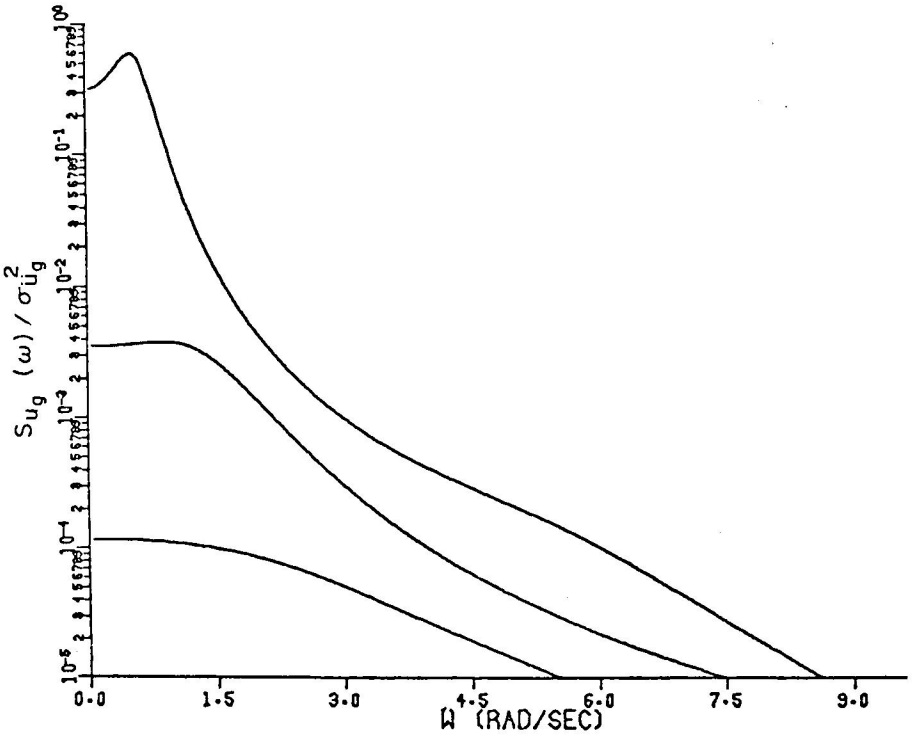

Figure 8 Spectra of Ground Displacement.

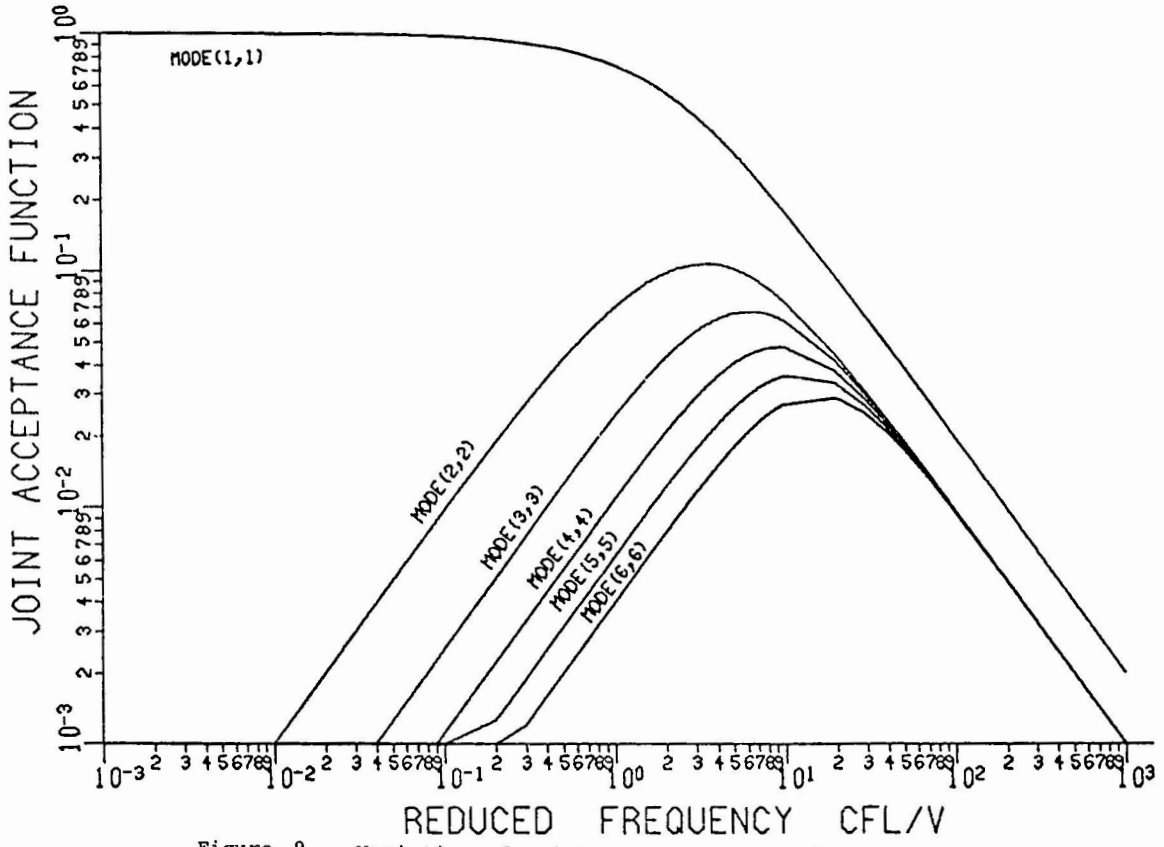

Figure 9 Variation of Joint Acceptance Function of a Soil-Pipe System $J_{j,k}(n)$ With Reduced Frequency n.

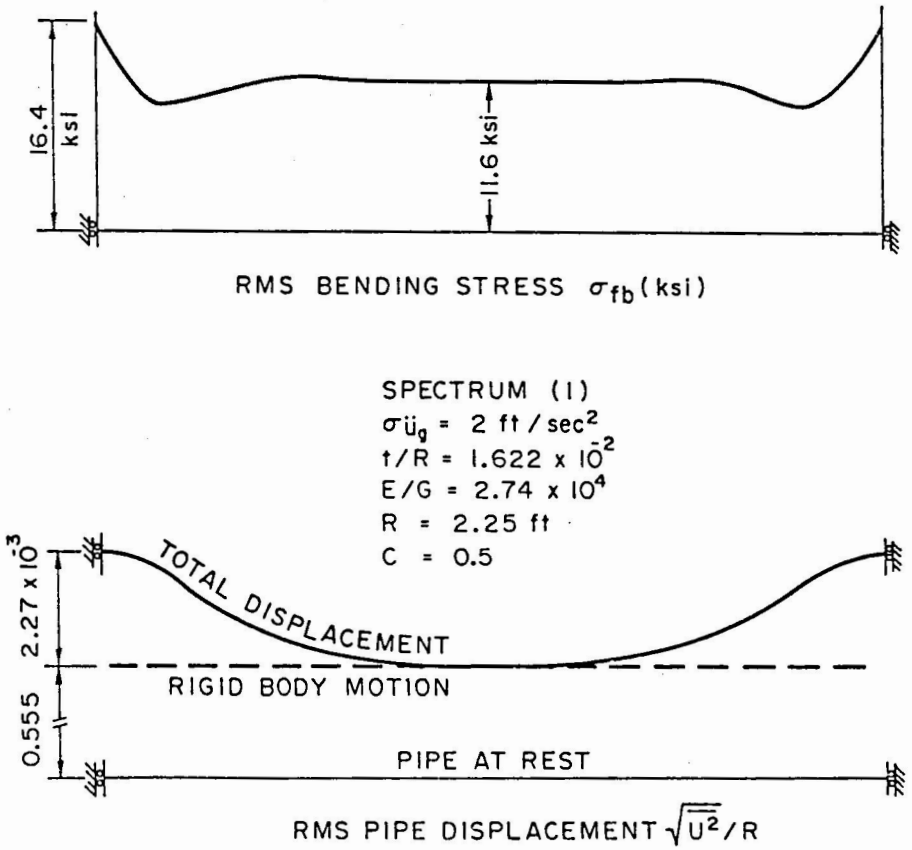

Figure 10 An Example of Pipe Lateral Response.

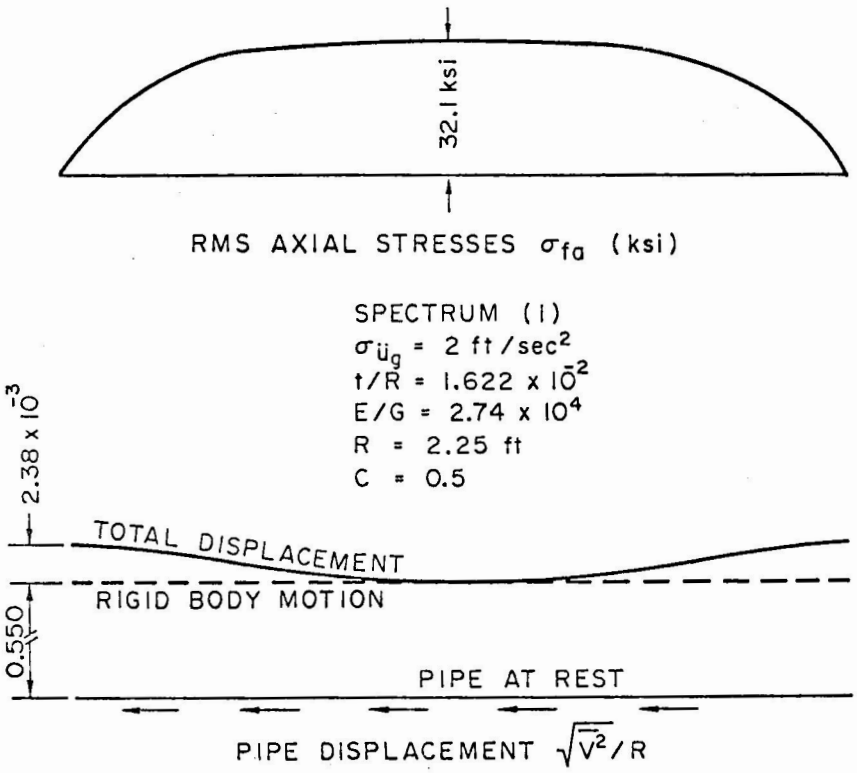

Figure 11 An Example of Pipe Axial Response.

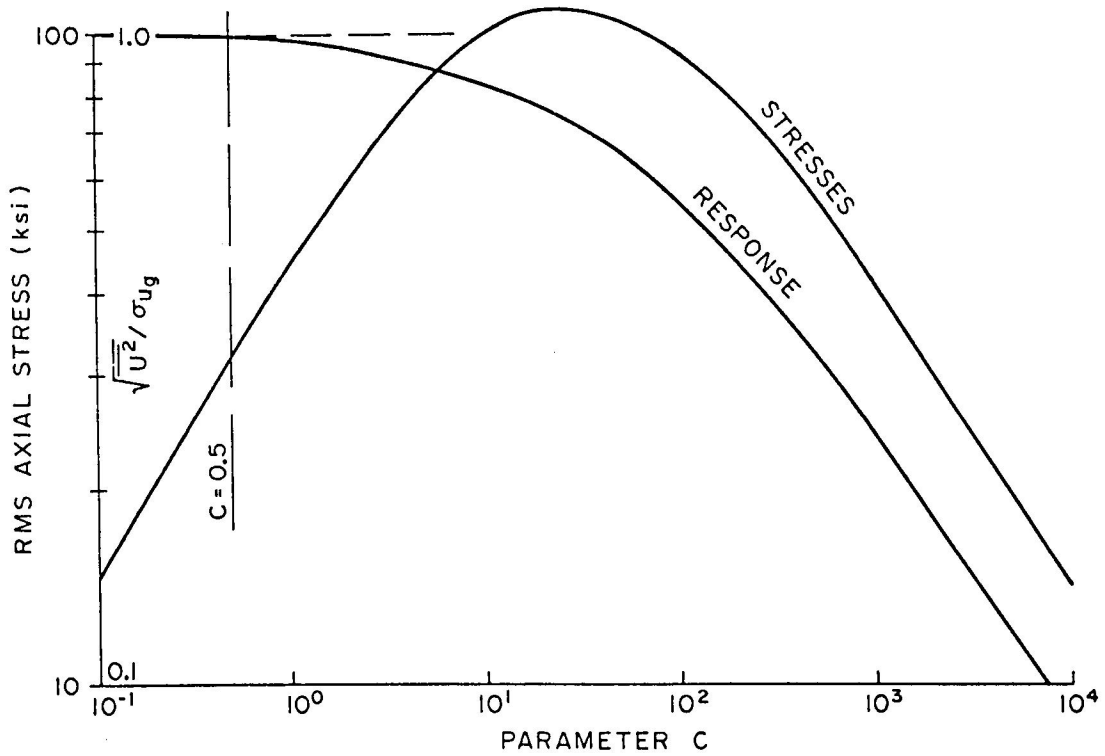

Figure 12 Variation of Pipe Response and Stresses With Parameter c.

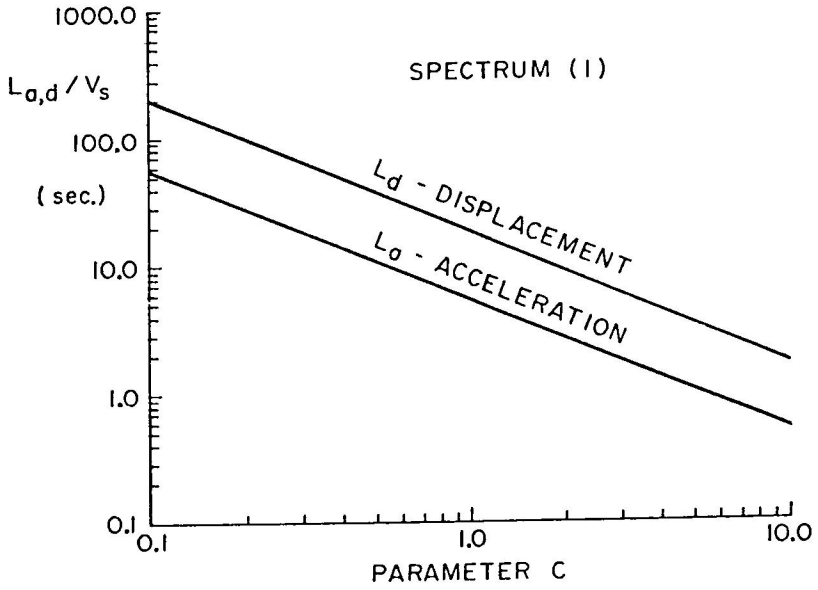

Figure 13 Variation of Wave Correlation Length With Parameter **c.**